

TABLE I Shrinkage in equilibrated and as-received samples

Time (min)	1100°C, $p_{O_2} \approx 10^{-4}$ atm.			
	Equilibrated		As received	
	$(\Delta L/L_0)$	$(\Delta L/L_0)^*$	$(\Delta L/L_0)$	$(\Delta L/L_0)^*$
5	0.0239	—	0.1560	—
10	0.0305	0.0066	0.1780	0.0220
50	0.0351	0.0112	0.1842	0.0282
100	0.0410	0.0171	0.1883	0.0323
200	0.0418	0.0179	0.1961	0.0401
500	0.0430	0.0191	0.1992	0.0432

Note: the incremental shrinkage $(\Delta L/L_0)^*$ is given as

$$\left(\frac{\Delta L}{L_0}\right)^* = \left(\frac{\Delta L}{L_0}\right) - \left(\frac{\Delta L}{L_0}\right)_{5 \text{ min.}}$$

concentration, would change with time. At low sintering temperatures, the equilibration would be imperceptibly slow and the change in defect concentration would occur only in the surface layer [16]. It is thus imperative that in the non-stoichiometric compounds, the equilibration and the sintering should be separately carried out in the correct atmosphere.

References

1. L. F. NORRIS and G. PARRAVANO, *J. Amer. Ceram. Soc.* **46** (1963) 449.
2. D. H. WHITMORE and T. KAWAI, *ibid* **45** (1962) 375.
3. K. W. LAY and R. E. CARTER, *J. Nuclear Mater.* **30** (1969) 74.

4. K. W. LAY, *J. Amer. Ceram. Soc.* **54** (1971) 18.
5. J. P. ROBERTS and J. HUTCHINGS, *Trans. Faraday Soc.* **55** (1959) 1394.
6. M. W. SHAFER, *J. Phys. Chem.* **65** (1961) 2055.
7. L. S. DARKEN and R. W. GURRY, *J. Amer. Chem. Soc.* **68** (1946) 798.
8. B. PHILLIPS and A. MUAN, *J. Phys. Chem.* **64** (1960) 1451.
9. Y. IIDA and S. OZAKI, *J. Amer. Ceram. Soc.* **42** (1959) 219.
10. C. E. BIRCHENALL, in "Mass Transport in Oxides" (NBS Special Publ. 296, Washington D.C., 1968) pp. 119-127.
11. S. J. BHATT and H. D. MERCHANT, *J. Amer. Ceram. Soc.* **52** (1969) 452.
12. R. L. COBLE, *J. Appl. Phys.* **32** (1961) 787.
13. M. J. BANNISTER, in "Sintering and Related Phenomena" (Gordon and Breach, New York, 1967) pp. 581-605.
14. S. M. KLOTSMAN, A. N. TIMOFEYEV and I. SH. TRAKHTENBERG, *Phys. Met. Metall.* **10** (5) (1960) 93.
15. L. C. F. BLACKMAN, *Ind. Chem.* **38** (1962) 620; **39** (1963) 23.
16. G. C. KUCZYNSKI, in "Powder Metallurgy in Nuclear Age" (Metallwerk Plansee, Reutte, Austria, 1962) pp. 166-79.

Received 29 January
and accepted 3 July 1973

D. W. STERNER
RCA Corp., Solid State Division.
Findley, Ohio, USA
H. D. MERCHANT
Indian Institute of Technology,
Kanpur, India

Transparent $Pb_{1-x}La_x(Hf_{1-y}Ti_y)O_3$ electro-optic ceramic

A number of compositions in the lead lanthanum zirconate-titanate (PLZT) solid solution series have been prepared as transparent ceramic materials and have been studied extensively in recent years on account of their potentially useful electro-optic properties [1, 2]. However, there have been few reports of the chemically similar lead hafnate-titanate series [3, 4] and none whatsoever on the system lead lanthanum hafnate-titanate (PLHT), the hafnate analogue of PLZT. In the past this neglect has been attributed to a combination of the relative scarcity of hafnium and the assumption that,

by virtue of the chemical similarity of hafnium and titanium, $PbHfO_3$ -based materials would behave identically to $PbZrO_3$ -based materials in all respects. However, since the hafnium atom is 1.95 times heavier than the zirconium atom whilst having virtually the same ionic radius, it seems likely that there may be substantial differences in phonon-dependent behaviour, e.g. optical and acoustic properties. This letter reports the preparation and preliminary evaluation of a transparent ceramic material having the composition $Pb_{0.90}La_{0.10}Hf_{0.65}Ti_{0.35}O_3$ (PLHT 10/65/35), being the hafnate analogue of a well-known electro-optic zirconate-based material (PLZT 10/65/35).

Transparent PLHT material was prepared in

TABLE I Dielectric properties of PLHT 10/65/35

	1kHz	10kHz	d.c.
Relative permittivity	2400	2190	—
Loss factor	0.05	0.07	—
Resistivity	—	—	$4 \times 10^{12} \Omega \cdot \text{m}$

polycrystalline ceramic form by standard techniques used in this laboratory and elsewhere. Appropriate weights of the oxides of lead, lanthanum, hafnium and titanium were blended in acetone for 8 h in a zirconia roller-ball mill, following which the resultant slurry was dried at 60°C. 20 g compacts, prepared by cold pressing at 155 MN m⁻², were hot-pressed in flowing oxygen at 1200°C, 31 MN m⁻² for 6 h using a programmed resistance-heated furnace and silicon nitride pressing tools. Samples for measurement were cut from the hot-pressed block using a diamond saw and polished to an optical finish.

The bulk density of the hot-pressed material, as determined by flotation in water, was 9.22 g cm⁻³; the residual porosity was too low to be determined by this technique. X-ray powder diffraction showed the material to have a cubic structure with a lattice parameter of 4.07 Å, giving good agreement between measured and calculated density and indicating that charge compensation for trivalent lanthanum takes place via the formation of A-site vacancies.

Dielectric properties were measured at frequencies of 1 and 10 kHz; in addition d.c. resistivity was also determined. The results are listed in Table I. In addition to room temperature measurements, the temperature dependence of the dielectric constant was determined. No sharp dielectric anomaly was observed between -40 and +200°C, instead, a very broad, low peak having a maximum in the vicinity of 48°C was recorded. Similar behaviour has been reported in the analogous PLZT composition [1].

Polished specimens of the material were transparent, with a distinct green-yellow colour. Fig. 1 shows the transmission for a 0.5 mm thick specimen in the visible and infra-red regions. Between 800 nm and 5.0 μm the transmission is constant at around 70%, Fresnel surface losses being responsible for the remaining 30%. This compares with the corresponding range in the PLZT material of 650 nm to 5.0 μm, also shown in Fig. 1. Above 2.0 μm the two materials show the same transmission. The refractive index at 633 nm, as deduced from transmission and

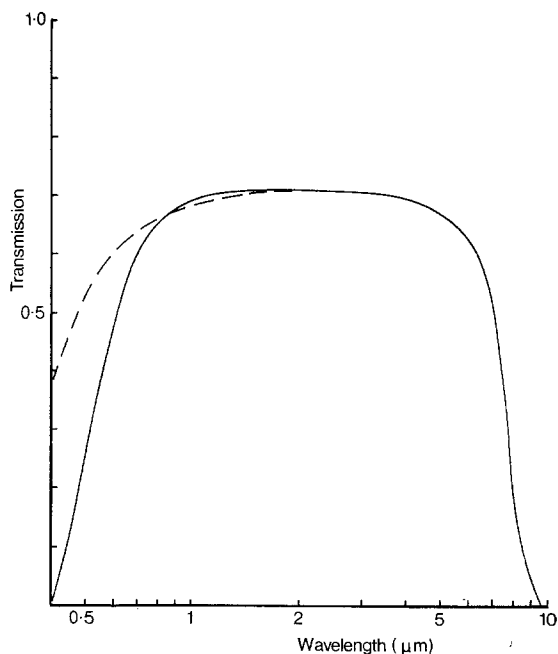


Figure 1 Optical transmission in zirconate and hafnate ceramic materials. Solid line: PLHT 10/65/35; broken line: PLZT 10/65/35.

reflection measurements [5], is 2.65, somewhat higher than the corresponding figure of 2.45 for PLZT at the same wavelength.

Electro-optic properties were measured on a 0.5 mm slice using a transverse field geometry with an inter-electrode gap of 1.0 mm. Measurements of field-dependent birefringence were made at 633 nm using a quartz wedge compensator; the quadratic electro-optic coefficient R was found to be $0.3 \times 10^{-16} \text{ m}^2 \text{ V}^{-2}$, compared with the figure of $0.7 \times 10^{-16} \text{ m}^2 \text{ V}^{-2}$ measured in the corresponding PLZT ceramic. When operated as a simple light "gate", a contrast ratio of better than 2000 was measured.

In general, the properties of the PLHT material resemble those of the corresponding PLZT composition. Although it is obviously unwise to generalize for a whole system on the basis of study of a single composition the dielectric constant and electro-optic coefficient results suggest that the PLHT 10/65/35 composition is slightly further away from the boundary between the ferroelectric and cubic phases than is the corresponding PLZT material. Confirmation of this point must await a fuller study of the phase diagram of this system.

We wish to thank the Directors of the Plessey Company Limited for permission to publish this paper.

References

1. G. H. HAERTLING and C. E. LAND, *J. Amer. Ceram. Soc.* **53** (1971) 1.
2. *Idem*, *Ferroelectrics* **3** (1972) 369.
3. B. JAFFE, R. S. ROTH and S. MARZULLO, *J. Res. N.B.S.* **55** (1955) 239.
4. C. A. HALL, R. H. DUNGAN and A. H. STARK, *J. Amer. Ceram. Soc.* **47** (1964) 259.

5. C. J. KIRKBY, *Ferroelectrics Conference Proceedings of the 3 IMF* (Edinburgh, 1973) (to be published).

F. W. AINGER
D. APPLEBY
C. J. KIRKBY

*Allen Clark Research Centre,
The Plessey Company Limited,
Caswell, Towcester, Northants, UK*

Received 16 February
and accepted 12 September 1973

Comments on "On the influence of deformation rate on intergranular crack propagation in Type 304 stainless steel"

I should like to dissent with some of the discussion of the paper by Nahm *et al* [1]. These authors present data relating to the growth characteristics of wedge cracks and infer that the growth rate depends on wedge height (rather than crack length) and that the angular orientation of the fastest growing cracks is also independent of crack length. This information is most useful but, unfortunately, in discussing it, the authors have tended to use an analysis, formulated by Evans [2], for the growth of grain-edge cavities. Such an approach is incorrect and leads to erroneous conclusions regarding the applicability of the cavity growth model.

My objection may best be summarized by reference to Figs 1 and 2. Fig. 1 represents schematically the geometry of a wedge crack growing along grain boundary A and fed by sliding on boundaries B and C to form a wedge of height (na). This is the type of crack found by Nahm *et al* for which an analysis by Williams [3] is applicable. He predicts that

$$\frac{\delta l}{\delta(na)} = \frac{\mu}{\pi(1-\nu)\sigma} \left\{ \left[1 - \frac{\sigma(na)}{2\gamma_p} \right]^{-\frac{1}{2}} - 1 \right\} \quad (1)$$

where μ is Poisson's ratio, σ is the applied normal stress and γ_p is the effective fracture energy. Clearly, from this equation, the growth process depends directly on the wedge height rather than on the crack length and this is entirely in accord with the observations of Nahm *et al*.

On the other hand, Evans' analysis relates only to the situation depicted in Fig. 2. Here a cavity lies on a single grain boundary D experien-

cing a sliding displacement, a , produced by the shear stress τ . The cavity growth relationship is [2]

$$\frac{\delta l}{\delta a} = \frac{\tau}{2\gamma_p NW} \left\{ 1 - \frac{\pi(1-\nu)\sigma_n^2 l}{8\mu\gamma_p} - \frac{\sigma_n h}{2\gamma_p} \right\}^{-1} \quad (2)$$

where N is the number of cavities per unit area of boundary, W is the average cavity width, h

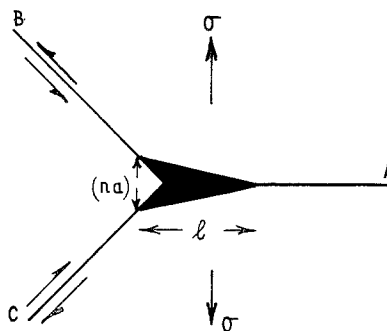


Figure 1 Wedge crack geometry.

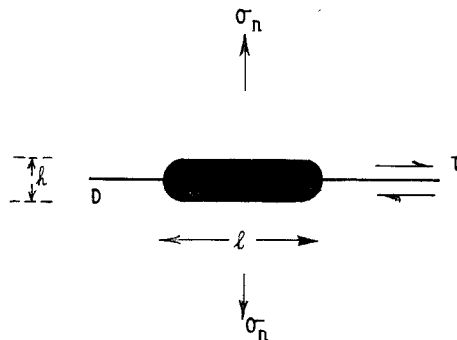


Figure 2 Cavity geometry.